



HAL
open science

Blood-brain barrier permeability is increased in normal appearing white matter in patients with lacunar stroke and leukoaraiosis

R Topakian, T R Barrick, F A Howe, H S Markus

► **To cite this version:**

R Topakian, T R Barrick, F A Howe, H S Markus. Blood-brain barrier permeability is increased in normal appearing white matter in patients with lacunar stroke and leukoaraiosis. *Journal of Neurology, Neurosurgery and Psychiatry*, 2010, 81 (2), pp.192. 10.1136/jnnp.2009.172072 . hal-00552765

HAL Id: hal-00552765

<https://hal.science/hal-00552765>

Submitted on 6 Jan 2011

HAL is a multi-disciplinary open access archive for the deposit and dissemination of scientific research documents, whether they are published or not. The documents may come from teaching and research institutions in France or abroad, or from public or private research centers.

L'archive ouverte pluridisciplinaire **HAL**, est destinée au dépôt et à la diffusion de documents scientifiques de niveau recherche, publiés ou non, émanant des établissements d'enseignement et de recherche français ou étrangers, des laboratoires publics ou privés.

Blood-brain barrier permeability is increased in normal appearing white matter in patients with lacunar stroke and leukoaraiosis

Topakian R, Barrick TR, Howe FA, Markus HS.

Clinical Neuroscience, St. George's University of London, London, UK

Corresponding author:

Professor Hugh S. Markus, Centre for Clinical Neuroscience, St George's University of London, Cranmer Terrace, London, SW17 0RE, UK.

E-mail hmarkus@sgul.ac.uk

Tel: +44 (0)20 8725 2735, Fax: +44(0)20 8725 2950

Word count: abstract 248, main text 3314.

Tables: 2.

Figures: 4.

References: 30.

Running Title: Blood brain barrier permeability in small vessel disease

Key Words: blood-brain barrier, cerebral small vessel disease, lacunar stroke, leukoaraiosis, magnetic resonance imaging

Acknowledgements: We are grateful to Rebecca Charlton and Francesca Schiavone for assistance with MR imaging and to Professor Joanna Wardlaw, Andrew Farrell, and Paul Armitage for helpful discussions on MRI methods and image analysis.

Abstract

Background and Purpose: The pathogenesis of cerebral small vessel disease (SVD) is incompletely understood. Endothelial dysfunction has been implicated and may result in increased blood-brain barrier (BBB) permeability with leakage of blood constituents into the vessel wall and white matter. We used contrast enhanced magnetic resonance imaging (MRI) to determine whether there was evidence for BBB permeability in the white matter of patients with SVD, and whether this was present not only in areas of leukoaraiosis (white matter lesions, WML) but also in normal appearing white matter (NAWM).

Methods: Subjects underwent T1 volumetric MRI before and after bolus injection of contrast. Scanning was continued for 30 minutes post injection to determine the contrast enhancement time course. Mean signal intensity change was plotted against time to calculate area under curve (AUC) values, a parameter related to BBB permeability. Automated brain segmentation and regions of interest analysis were performed to determine “permeability” in different brain compartments.

Results: Compared to controls (n=15), the SVD patient group (n=24) had signal changes consistent with increased BBB permeability in NAWM ($P = 0.033$). Multivariate regression analyses identified leukoaraiosis grade as an independent predictor of these permeability related signal changes in NAWM after adjustment for age, gender, weight, brain volume, AUC in the internal carotid arteries, and cardiovascular risk factors.

Conclusion: This study provides evidence for increased BBB permeability in SVD, and this is particularly seen in SVD with leukoaraiosis. Its presence in NAWM would be consistent with it playing a causal role in disease pathophysiology.

Introduction

Cerebral small vessel disease (SVD) causes lacunar stroke which accounts for a quarter of ischaemic stroke¹ and is a major cause of vascular dementia.² Despite its importance the underlying pathogenesis is poorly understood. Radiologically, small lacunar infarcts are seen with or without more diffuse regions of white matter lesions (WML), referred to as leukoaraiosis, and best seen as high signal on T2- or fluid attenuated inversion recovery (FLAIR) sequences.³ Two clinicopathological phenotypes of SVD have been hypothesised: multiple small lacunar infarcts with leukoaraiosis associated with diffuse small vessel changes on pathology, and single or a few larger lacunar infarcts without leukoaraiosis associated with perforator vessel atherosclerosis.^{4,5}

Considerable evidence suggests that, particularly for the leukoaraiosis phenotype, endothelial dysfunction plays a role in pathogenesis. Endothelial abnormalities have been shown on pathology.⁶ Circulating blood markers of endothelial activation are elevated, particularly in the leukoaraiosis variant.^{7,8} Such endothelial dysfunction could predispose to tissue damage via reduced cerebral blood flow and impaired autoregulatory responses; such abnormalities have been reported in SVD.^{9,10}

In addition, endothelial dysfunction could cause blood brain barrier (BBB) permeability increase.¹¹ This has been hypothesised to result in leakage of plasma components into the vessel wall and surrounding brain tissue, contributing to vessel wall damage and brain parenchymal damage, the latter resulting in leukoaraiosis.^{11,12} Consistent with BBB breakdown, immunohistochemical studies found extravasation of serum proteins.¹³ Furthermore, increased cerebrospinal fluid (CSF)/serum albumin ratio, a marker of BBB breakdown, was reported in vascular dementia.^{14,15} However this technique does not allow

regional variations in BBB breakdown, and differences between lesioned and normal appearing white matter (NAWM), to be determined.

Recently, contrast enhanced magnetic resonance imaging (MRI) has been used to study BBB permeability.¹⁶⁻¹⁹ An early study in vascular dementia suggested increased permeability, although another early study failed to replicate this finding.^{16,17} A recent study reported increased permeability in the white matter of lacunar stroke patients compared with cortical stroke patients.¹⁹ No studies have been performed using an automated analysis to determine permeability both within and outside WML. Within areas of leukoaraiosis any increase in permeability could be a secondary consequence of tissue damage. If increased permeability plays a causal role in pathogenesis, one might expect to detect increased permeability not only in areas of leukoaraiosis, but also in NAWM. Previous studies have not related permeability to the SVD phenotype, and the presence of leukoaraiosis. If endothelial dysfunction is primarily important in patients with the leukoaraiosis subtype, one might expect BBB permeability to be related to the presence of leukoaraiosis.

We used MRI, with prolonged imaging following contrast injection, and determined MRI signal intensity changes that may relate to alterations in BBB permeability, both in NAWM and WML, in SVD, and normal controls. We examined the hypothesis that increased permeability would be related to the degree of leukoaraiosis, and would be present not only within WML, but also in NAWM.

Methods

Subjects

28 SVD patients were recruited. Inclusion criteria were a classical lacunar syndrome (pure motor stroke, pure sensory stroke, sensorimotor stroke, or ataxic hemiparesis/clumsy hand dysarthria) with a compatible lacunar infarct on MRI. All patients were assessed by a consultant neurologist. Patients were included in the study at least 6 weeks post last stroke or TIA to reduce the effect of acute ischaemia on permeability. Exclusion criteria were: age <18 years, stroke cause other than SVD (cardioembolic source, stenosis >50% in any extracranial or intracranial large artery, any cortical infarct, any subcortical infarct >1.5cm diameter), and any contraindication to MRI. 21 controls without any history of stroke, central nervous system disease, or any other disease associated with white matter damage, were also recruited. These were spouses of patients and volunteers from a community based study of normal ageing.

The study was approved by the local research ethics committee. All subjects gave written informed consent.

MRI scanning procedure

All MRI scanning was performed on a GE 1.5 T Signa LX scanner equipped with 22mT/m EchoSpeed gradients running 8x software (General Electric, Milwaukee, Wisconsin, USA). MRI included sagittal T1 weighted, axial FLAIR, high-resolution coronal 3D-fast spoiled gradient echo (3D-FSPGR), T1 weighted, and axial 3D-FSPGR T1 weighted sequences. The high resolution coronal 3D-T1 weighted imaging was used for image segmentation (TR/TE fixed at 11.1/5 ms, 1.1 mm slice thickness, no slice gap, field of view 28x28 cm, matrix 256x192, 176 slices). The imaging technique was similar to that used previously identify

evidence of BBB permeability changes.¹⁹ For the dynamic contrast study an axial 3D-FSPGR with flip angle at 12 degrees was used (TR/TE 7.3/3.4 ms, 4 mm slice thickness, no slice gap, field of view 24x24 cm, matrix 256x256, 36 slices). The axial 3D-FSPGR T1 weighted imaging was used in a continuous multiphase mode, providing 36-slice images of the whole head at 27 time points over a 29min 6sec acquisition time. A bolus of a gadolinium based contrast agent (Omniscan®, GE Healthcare Medical Diagnostics, Bucks, United Kingdom) was injected intravenously at a fixed dose of 40mL per patient (5mL/sec) after the first image in this series. To correct for any scanner signal intensity drift, we used a linear mathematical correction derived from the MRI data of 11 healthy young subjects who underwent the 3D T1 weighted sequences without contrast application.

Image analysis

MRI data were analyzed on an independent workstation (Sun Blade 100; Sun Microsystems, Mountain View, USA).

Quantification of white matter lesions and atrophy

WML load was determined using both a semi-quantitative scale and a semi-automated programme. The semi-quantitative Fazekas scale was used,²⁰ with all scans being reviewed by the same experienced rater blinded to the permeability imaging results. An additional category was included to allow differentiation of more severe cases of leukoaraiosis. Leukoaraiosis was therefore rated as: 0 = absent; 1 = mild; 2 = early confluent; 3 = severe confluent.

For each patient, a “WML mask” containing all WML was constructed by application of a semi-automatic region extraction technique using the contour function in the Dispunc image display program (David Plummer, University College London, UK) to delineate the contours of areas of WML observed on FLAIR images.

To adjust for atrophy, brain tissue volume, normalised for subject head size, was estimated using SIENAX.^{21,22}

Brain segmentation

Using the high resolution T1 weighted images and the WML mask derived from FLAIR images, automatic brain segmentation was computed for each individual (Fig. 1). Firstly, the T1 weighted images were segmented into grey matter, white matter, and CSF tissue maps, incorporating a correction for image intensity non-uniformity in SPM2,²³ Secondly the T1-weighted and FLAIR images were co-registered (using a 12-parameter affine transformation) to the precontrast 3D T1 weighted images in SPM2. These transformations were applied to the WML mask and the segmented images to co-register them to the precontrast 3D T1 weighted images. Thirdly, hard segmentations of the co-registered segmented images were computed such that each image voxel was assigned to a single tissue class according to thresholds of intensity values defining the highest likelihood probability of each voxel belonging to the tissue types. The co-registered WML mask was then overlain on the hard segmentations to generate a brain mask image representing WML and NAWM at each image voxel.

Analysis of dynamic contrast imaging data

For each of the 27 time-points after contrast injection the 3D T1-weighted images were aligned to the same image prior to gadolinium injection using a 12-parameter affine transformation in FLIRT (FSL tools <http://www.fmrib.ox.ac.uk/fsl/>).²⁴ Percentage signal change between the T1-weighted intensities pre- and post-contrast injection was computed at every voxel of each of the 27 time-points. Using the brain mask computed from the FLAIR and high resolution T1-weighted images the signal intensity change was determined in each of the segmented compartments of the brain. Mean percentage signal intensity change for each

compartment was then plotted against time to calculate area under curve values (AUC) over the full time course of dynamic imaging as a robust model-independent measure to detect differences in the vascular characteristics of each patient with high sensitivity.

Although signal intensity measurements over large volumes of a single tissue type increase sensitivity to detect small signal changes, tissue segmentation may not perfectly separate tissue signal from that of large blood vessels. To reduce partial volume effects we also calculated the difference between average signal changes for control and patient data at each time point, on the assumption that the large vascular structures in the two groups would be similar hence partial volume effects would cancel. In addition this difference measurement also allows cancellation of systematic errors from drift in scanner sensitivity that occurs over a long acquisition period.

Regions of interest analysis in the internal carotid arteries

Because slower washout of the contrast agent could reflect BBB damage but just as well slowed tracer clearance due to e.g. impaired renal function, we assessed AUC in the internal carotid arteries of each individual by manually placing small regions of interest (ROI) over the internal carotid arteries as suggested and performed by Wardlaw et al.¹⁹ The ROI arterial blood data were included in the multivariate analyses (outlined below) to adjust for arterial tracer concentration.

Statistical analysis

For univariate analyses of categorical variables, we used two-tailed Fisher's Exact test or Pearson's chi-square test as appropriate. For continuous variables, differences between groups were assessed by the two-tailed independent samples t-test (data with normal distribution), Mann-Whitney U test (skewed data, 2 groups) and Kruskal-Wallis test (skewed

data, >2 groups). Correlation of continuous variables was tested using Spearman's rho. To identify independent predictors of changes in the AUC (i.e. the post-contrast signal characteristic) in NAWM and cerebrospinal fluid, multivariate regression analyses were performed by entering the following variables into the model: age, gender, weight, brain volume, leukoaraiosis grade, AUC in the internal carotid arteries, presence of hypertension, presence of diabetes, and current smoking. *P* values <0.05 were considered to be statistically significant. SPSS software (Version 14.0, SPSS, Chicago, USA) was used for all analyses.

Results

Baseline characteristics

Baseline characteristics are given in Table 1. Four patients were excluded prior to image analysis; one because post-contrast scanning had to be stopped immediately after injection of gadolinium due to severe nausea; two due to movement artefacts and poor image quality; one due to incomplete post-contrast T1 acquisition due to technical reasons. This left 24 patients for analysis. Three of the 21 controls were excluded; due to movement artefacts and poor image quality in two, and incomplete post-contrast T1 acquisition for technical reasons in one. Three further controls were excluded because they had confluent leukoaraiosis (grade 2). Therefore 15 controls were included in analysis.

Demographic characteristics are shown in table 1. There was no difference in mean (SD) age between cases and controls (67.1(±8.9) and 65.5(±6.7) respectively) or in gender or weight. Hypertension and hypercholesterolaemia were more common in cases (Table 1). In patients, the median time delay between MRI and the last TIA or stroke was 12 months (range 1.5–56).

Kinetics of signal intensity change

The average kinetics of signal intensity change in white matter in both cases and controls are shown in Fig. 2 and are similar to that expected from changes in plasma contrast agent concentration.²⁵ The difference plots in Fig. 3 demonstrate differences between control and patient long time constant kinetics for NAWM, but not for WML. The increase in the signal intensity difference between patients and controls for NAWM are suggestive of the greater accumulation of contrast in the patient group compared to controls, in whom the contrast agent is not expected to cross the BBB, and therefore suggests increased leakage.

Patients had significantly higher AUC values for NAWM compared to controls (Mann-Whitney U , median; range: 1.0; 0.23–1.65 vs. 0.76; 0.3–1.36; $P=0.033$) but there was no difference for WML ($P=0.966$), ICA ($P=0.172$) and CSF ($P=0.258$). In patients, there was no correlation of the time from the last stroke or TIA event and the signal intensity change for NAWM (Spearman's $\rho=-0.064$, $P=0.82$).

Analysis according to leukoaraiosis grade

To study the relationship between AUC and degree of leukoaraiosis, subjects were assigned to the following four groups: controls with LA grade 0-1 ($n=15$); patients with LA grade 0-1 ($n=8$); patients with LA grade 2 ($n=6$); and patients with LA grade 3 ($n=10$). Kruskal-Wallis tests comparing AUCs between groups (Fig. 4) showed that higher grade of LA was associated with increased AUC in NAWM ($P=0.039$) but there was no trend across subgroups for WML ($P=0.641$).

Determinants of contrast agent leakage

Multiple regression analyses were performed to assess the relationship between clinical variables and AUC in NAWM and CSF in the whole dataset (Table 2). After controlling for

age, gender, weight, brain volume, AUC in the internal carotid arteries, hypertension, diabetes, and current smoking, leukoaraiosis grade was found to be an independent predictor of leakage as represented by the AUC in NAWM ($P=0.027$) and in CSF ($P=0.001$) (Table 2).

Discussion

We have applied a sensitive MRI technique to investigate small differences in global perfusion and permeability characteristics of brain tissue. Furthermore, we used an image segmentation technique to generate tissue masks from which post-contrast AUCs were computed of signal intensity change over an extended time period. Comparison of AUC provides an estimate of blood brain barrier permeability alterations.

Our results are consistent with increased BBB permeability in the white matter of patients with SVD. The AUC in NAWM was greatest in those SVD patients with leukoaraiosis, and there was a positive correlation between AUC and degree of leukoaraiosis. This supports the hypothesis that BBB permeability is particularly important in the leukoaraiosis subtype of SVD. These correlations persisted after controlling for conventional cardiovascular risk factors, and on multivariate analysis leukoaraiosis grade remained a significant determinant of AUC. A relationship was also found between leukoaraiosis grade and CSF AUC, consistent with increased contrast leakage into the CSF in the presence of more severe leukoaraiosis.

We used an automated segmentation approach to separately determine AUC in established WML and in NAWM. We found a progressive increase in AUC in the NAWM of the patient group with leukoaraiosis grade. This would be consistent with increased permeability preceding the development of WML lesions and thus playing a causal role. Once developed,

WML in both symptomatic and asymptomatic subjects had similar permeability characteristics as described by the AUC.

In the signal intensity with time plots (Fig. 2), there is initially a step increase, followed by a slow decay. Such a pattern is characteristic of a large post-contrast signal intensity increase due to the vascular compartment of the signal, followed by a decline due to a combination of contrast wash-out and contrast leakage into the tissue compartment of the signal. For NAWM there are significant differences between patients and controls in the difference plots (Fig. 3) and the AUC (Fig. 4) due to changes with a long time constant. As no differences between the two groups were observed in brain volume (Table 1) or in initial signal intensity changes (Fig. 3), it is unlikely that group differences in tissue/vascular partial volume are responsible for the observed group differences in AUC. Consequently, the greater AUC for NAWM in patients compared to controls is more consistent with an accumulation of contrast agent due to increased leakage out of the vascular space. However, although the AUC is a sensitive and model independent measurement, its interpretation is not without ambiguity²⁷. In particular, simulations show that the AUC will increase with increased permeability, increased extra-cellular extra-vascular space or increased blood flow.²⁸ Increased blood flow is unlikely to be an explanation for our findings. Patients with the highest AUC were those with the most severe leukoaraiosis and cerebral blood flow is reduced in the NAWM in this group.⁹ Therefore increased blood flow is an unlikely candidate for explaining the signal differences between patients and controls in NAWM. Furthermore, in a previous study with a similar acquisition protocol, signal enhancement declined more rapidly in the blood compared to the brain, and CSF signal enhancement (uncontaminated by intravascular enhancement) was quite different to that of the blood.¹⁹ Previous studies using diffusion weighted imaging have shown an increase in apparent diffusion coefficients in normal white matter of patients with leukoaraiosis,²⁹ which could be interpreted as an increase in the extra-cellular space.

However, the post-mortem characteristics of leukoaraiosis are of axonal loss accompanied by gliosis, factors which provide an explanation for the increased median diffusivity previously observed,²⁹ but with no change in extra-cellular space.³⁰

An alternative potential explanation could be that slower washout of contrast merely reflects slowed tracer clearance, for example due to impaired renal function in patients with leukoaraiosis. To control for this we measured signal intensity in the arterial compartment by placing regions of interest in the carotid artery. The associations persisted after controlling for this, suggesting slower tracer clearance does not account for the differences we observed.

We used a fixed dose of contrast rather than a weight adjusted dose. However differences between cases and controls, and the relationships between AUC and leukoaraiosis grade persisted after including weight in the multivariate regression. However future studies should include weight adjusted contrast doses.

Our findings are consistent with results obtained in previous studies using biochemical techniques, primarily those measuring CSF/serum albumin ratios in order to identify increased BBB permeability. A recent meta-analysis concluded that, while studies were disparate and individually gave conflicting results, the overall data suggested that BBB permeability is increased in vascular dementia, for which SVD is a major cause.²⁶ Data was more limited from patients with MRI identified WML, but was consistent with increased BBB permeability. However, the CSF/serum albumin technique does not allow regional differences in permeability to be determined, and differentiation of whether the increased permeability is a secondary phenomenon to tissue damage in WML, or an early phenomenon occurring in NAWM.

The few previous studies using MRI have given conflicting results. A small study on 10 demented patients with WML failed to detect differences in contrast enhancement of WML and NAWM between patients with and without elevated CSF/serum albumin ratio.¹⁶ However, the sample size was not powered to detect moderate differences. In 17 subjects with Binswanger's disease permeability within WML was greater than in non-demented subjects (10 with cerebrovascular disease and 14 controls).¹⁷ Recently, using a similar acquisition technique to that used in our study, BBB permeability was significantly higher in the CSF of patients with lacunar compared to cortical stroke.¹⁹ There was a non-significant increase in white matter permeability. No differences were found in the grey matter. However the cortical stroke control group obviously had cortical pathology, and this may have obscured any increased GM permeability in the lacunar stroke group.

Previous MRI studies, with one exception,¹⁷ have not determined permeability separately in WML and NAWM. They have also not determined whether there may be differences in permeability between the different subtypes of SVD, and whether increased permeability is primarily seen in the leukoaraiosis phenotype. Our data not only show clear differences in leakage characteristics between lesioned and non lesioned white matter, but also suggest increased permeability in NAWM, supporting the hypothesis that (widespread) increased BBB permeability may be a potential pathomechanism by which tissue damage can occur. A primary disease causal event could be alteration of cerebral microvascular endothelial (i.e. BBB) function. This could result in extravasation of plasma components into the arteriolar wall (causing the wall thickening, cellular infiltration, disintegration and perivascular damage seen pathologically) and the leakage into the adjacent brain parenchyma causing "perivascular oedema-related lesions" which are then seen radiologically as leukoaraiosis.¹¹

In conclusion, this study provides evidence consistent with increased BBB permeability in NAWM of SVD subjects with leukoaraiosis. These findings are consistent with increased BBB permeability playing a causal role in disease pathogenesis. Further data is required from larger studies to confirm these findings. However only longitudinal studies using consistent quantitative contrast-enhanced MRI approaches in large enough numbers of subjects can determine whether BBB permeability in NAWM predicts the future development of WML in areas of abnormal leakage. If it indeed plays a causal role in disease this may offer new treatment approaches.

References

1 Bamford J, Sandercock P, Dennis M, Burn J, Warlow C. Classification and natural history of clinically identifiable subtypes of cerebral infarction. *Lancet*. 1991; 337: 1521–1526.

2 Garde E, Mortensen EL, Krabbe K, Rostrup E, Larsson HB. Relation between age-related decline in intelligence and cerebral white-matter hyperintensities in healthy octogenarians: a longitudinal study. *Lancet*. 2000; 356: 628–634.

3 Hachinski VC, Potter P, Merskey H. Leuko-araiosis: an ancient term for a new problem. *Can J Neurol Sci*. 1986; 13 (Suppl 4): 533–534.

4 Fisher CM. The arterial lesions underlying lacunes. *Acta Neuropathol*. (Berl) 1968; 12: 1–15.

5 Boiten J, Lodder J, Kessels F. Two clinically distinct lacunar infarct entities? A hypothesis. *Stroke*. 1993; 24: 652–656.

6 Fernando MS, Simpson JE, Matthews F, et al. White matter lesions in an unselected cohort of the elderly: molecular pathology suggests origin from chronic hypoperfusion injury. *Stroke*. 2006; 37, 1391–1398.

7 Hassan A, Hunt B, O'Sullivan M, et al. The role of endothelial dysfunction in lacunar infarction and ischaemic leukoaraiosis. *Brain*. 2003; 126: 424–432.

8 Markus HS, Hunt B, Palmer K, Enzinger C, Schmidt H, Schmidt R. Markers of endothelial and haemostatic activation and progression of cerebral white matter hyperintensities: longitudinal results of the Austrian Stroke Prevention Study. *Stroke*. 2005; 36: 1410–1414.

9 O'Sullivan M, Lythgoe DJ, Pereira AC, et al. Patterns of cerebral blood flow reduction in patients with ischemic leukoaraiosis. *Neurology*. 2002; 59: 321–326.

10 Terborg C, Gora F, Weiller C, Röther J. Reduced vasomotor reactivity in cerebral microangiopathy: a study with near-infrared spectroscopy and transcranial Doppler sonography. *Stroke*. 2000; 31: 924–929.

11 Wardlaw JM, Sandercock PAG, Dennis MS, Starr J, Kalimo H. Is breakdown of the blood–brain barrier responsible for lacunar stroke, leukoaraiosis, and dementia? *Stroke*. 2003; 34: 806–812.

12 Wardlaw JM. What causes lacunar stroke? *J Neurol Neurosurg Psychiatry*. 2005; 76: 617–619.

13 Tomimoto H, Akiguchi I, Suenaga T, et al. Alterations of the blood-brain barrier and glial cells in white-matter lesions in cerebrovascular and Alzheimer's disease patients. *Stroke*. 1996; 27: 2069–2074.

14 Wallin A, Blennow K, Fredman P, Gottfries CG, Karlsson I, Svennerholm L. Blood brain barrier function in vascular dementia. *Acta Neurol Scand*. 1990; 81: 318–322.

15 Skoog I, Wallin A, Fredman P, et al. A population study on blood-brain barrier function in 85-year-olds: relation to Alzheimer's disease and vascular dementia. *Neurology*. 1998; 50: 966–971.

16 Wahlund LO, Bronge L. Contrast-enhanced MRI of white matter lesions in patients with blood-brain barrier dysfunction. *Ann N Y Acad Sci*. 2000; 903: 477–481.

17 Hanyu H, Asano T, Tanaka Y, Iwamoto T, Takasaki M, Abe K. Increased blood-brain barrier permeability in white matter lesions of Binswanger's disease evaluated by contrast-enhanced MRI. *Dement Geriatr Cogn Disord*. 2002; 14: 1–6.

18 Starr JM, Wardlaw J, Ferguson K, MacLulich A, Deary IJ, Marshall I. Increased blood-brain barrier permeability in type II diabetes demonstrated by gadolinium magnetic resonance imaging. *J Neurol Neurosurg Psychiatry* 2003; 74: 70–76.

19 Wardlaw JM, Farrall A, Armitage PA, et al. Changes in background blood-brain barrier integrity between lacunar and cortical ischemic stroke subtypes. *Stroke*. 2008; 39: 1327–1332.

20 Fazekas F, Chawluk JB, Alavi A, Hurtig HI, Zimmerman RA. MR signal abnormalities at 1.5 T in Alzheimer's dementia and normal aging. *AJR Am J Roentgenol*. 1987; 149: 351–356.

21 Smith SM, Zhang Y, Jenkinson M, et al. Accurate, robust, and automated longitudinal and cross-sectional brain change analysis. *Neuroimage*. 2002; 17: 479–489.

22 Smith SM, Jenkinson M, Woolrich MW, et al. Advances in functional and structural MR image analysis and implementation as FSL. *Neuroimage*. 2004; 23 (Suppl 1): S208–219.

23 Ashburner J, Friston KJ. Voxel-based morphometry - the methods. *Neuroimage*. 2000; 11: 805–821.

24 Jenkinson M, Bannister PR, Brady JM, Smith SM. Improved optimization for the robust and accurate linear registration and motion correction of brain images. *Neuroimage*. 2002; 17: 825–841.

25 Tofts PS, Kermode AG. Measurement of the blood-brain barrier permeability and leakage space using dynamic MR imaging. 1. Fundamental concepts. *Magn Reson Med*. 1991;17: 357–367.

26 Farrall AJ, Wardlaw JM. Blood-brain barrier: Ageing and microvascular disease - systematic review and meta-analysis. *Neurobiol Aging*.
doi:10.1016/j.neurobiolaging.2007.07.015

27 Evelhoch JL. Key factors in the acquisition of contrast kinetic data for oncology. *J Magn Reson Imaging*. 1999; 10: 254–259.

28. Walker-Samuel S, Leach MO, Collins DJ. Evaluation of response to treatment using DCE-MRI: the relationship between initial area under the gadolinium curve (IAUGC) and quantitative pharmacokinetic analysis. *Phys. Med. Biol*. 2006; 51: 3593–3602.

29. Helenius J, Soenne L, Salonen O, Kaste M, Tatlisumak T. Leukoaraiosis, ischemic stroke, and normal white matter on diffusion-weighted MRI. *Stroke*. 2002; 33:45–50.

30. Jones DK, Lythgoe D, Horsfield MA, Simmons A, Williams SCR, Markus HS.
Characterisation of white matter damage in ischaemic leukoaraiosis with diffusion tensor
magnetic resonance imaging. *Stroke* 1999; 30: 393-397

Table 1: Baseline characteristics. Values are means (\pm SD) or subject numbers (percentages).

[†] independent samples t-test; ^{††} Fisher's Exact test; ^{†††} Pearson's chi-square test

	Patients (n = 24)	Controls (n = 15)	<i>P</i>
Age, years	67.1 (\pm 8.9)	65.5 (\pm 6.7)	0.566 [†]
Weight, kg	79.5 (\pm 21.3)	72.8 (\pm 12.8)	0.225 [†]
Male sex	16 (66.7%)	9 (60%)	0.74 ^{††}
Hypertension	21 (87.5%)	2 (13.3%)	<0.0005 ^{††}
Diabetes	6 (25%)	0	0.065 ^{††}
Hypercholesterolaemia	18 (75%)	6 (40%)	0.044 ^{††}
Current smoker	7 (29.2%)	3 (20%)	0.711 ^{††}
Ischaemic heart disease	3 (12.5%)	2 (13.3%)	1.0 ^{††}
Leukoaraiosis grade			
0	4 (16.7%)	11 (73.3%)	
1	4 (16.7%)	4 (26.7%)	
2	6 (25%)	0	
3	10 (41.7%)	0	<0.0005 ^{†††}

Table 2: Multiple regression model to identify determinants of increased blood-brain barrier permeability in normal appearing white matter (NAWM) and cerebrospinal fluid (CSF).

	NAWM		CSF	
R square	0.494		0.603	
ANOVA				
F	3.144		4.897	
P	0.009		< 0.0005	
Variables	Beta	P	Beta	P
Age	-0.138	0.492	-0.293	0.105
Gender	0.04	0.79	-0.185	0.166
Weight	-0.551	0.007	-0.085	0.619
Brain volume	-0.04	0.821	0.18	0.257
Leukoaraiosis grade	0.364	0.027	0.542	0.001
AUC in ICA	-0.134	0.459	0.233	0.152
Hypertension	0.232	0.164	-0.001	0.995
Diabetes	-0.017	0.913	-0.124	0.369
Current smoking	0.112	0.5	0.204	0.172

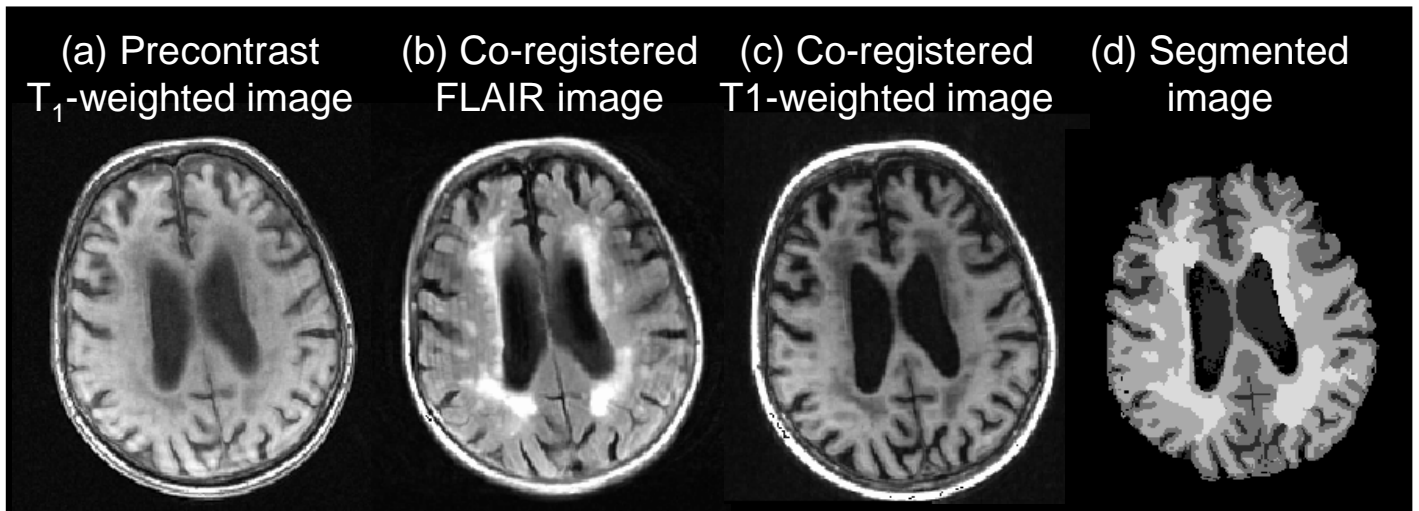


Figure 1: Automatic segmentation technique. The precontrast T1-weighted image (a) was used as the target image for co-registration of the FLAIR (b) and high resolution T1-weighted image (c). The final brain mask for the patient (d) is shaded according to tissue classification (dark grey – CSF, mid-grey – grey matter, light grey – normal appearing white matter, white – lesion).

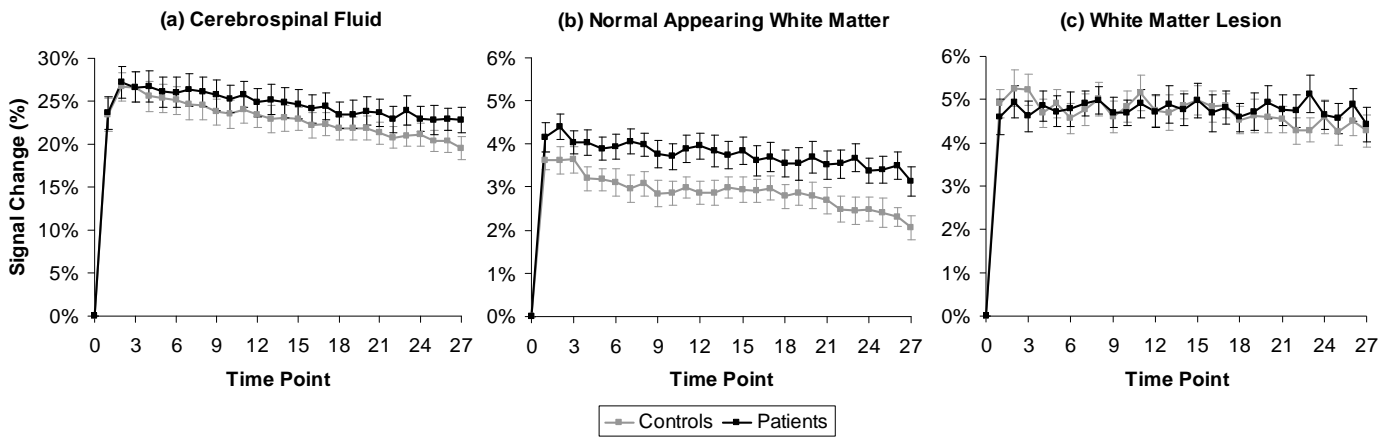


Figure 2: Kinetics of post-contrast signal intensity change over time in patients and controls in the cerebrospinal fluid (graph a), normal appearing white matter (graph b), and white matter lesions (graph c). Standard error bars are marked on the graphs.

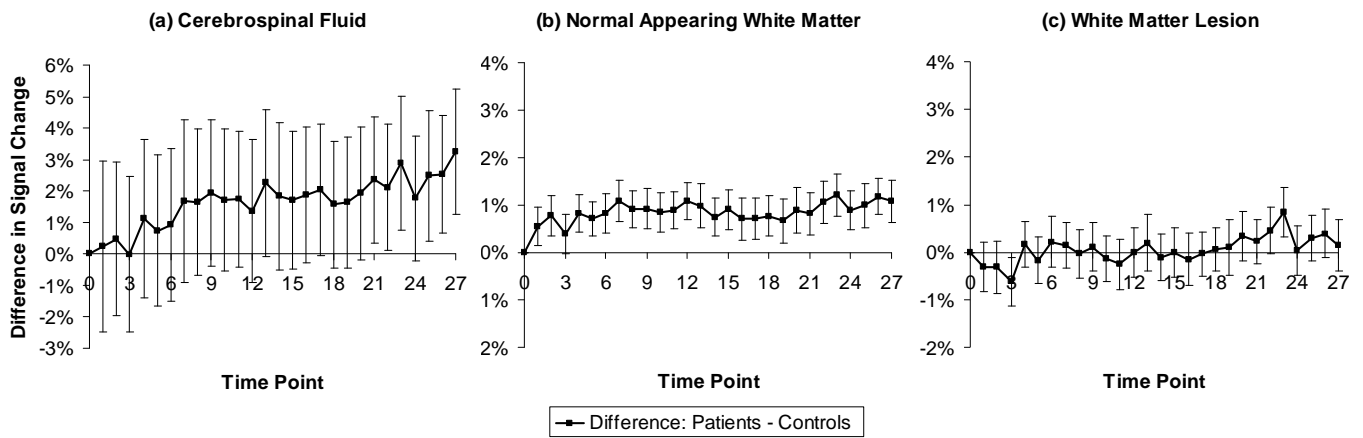


Figure 3: Kinetics of the post-contrast signal changes shown as the difference between the signal averages of the control and patient group data shown in Fig. 3 for cerebrospinal fluid (graph a), normal appearing white matter (graph b) and white matter lesions (graph c). Error bars represent the square root of the sum of squares of the standard errors on the patient and control groups.

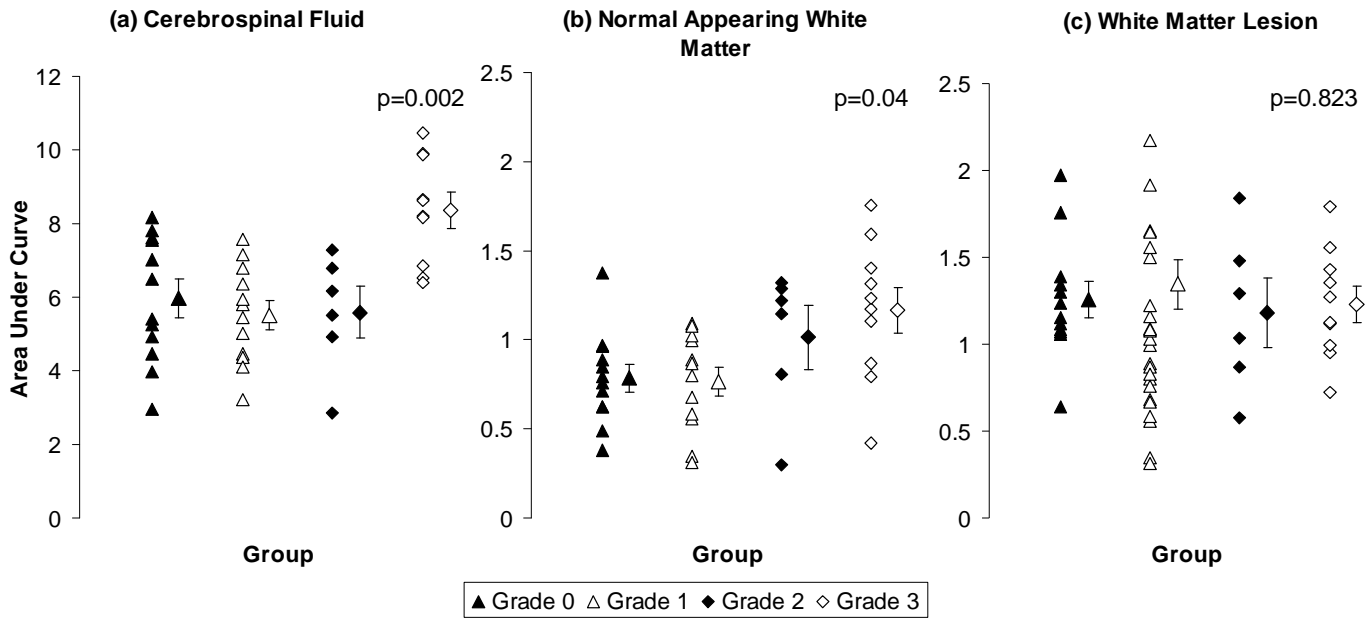


Figure 4: Plots of area under curves (AUC) of post-contrast signal intensity change in subgroups according to leukoaraiosis grade and subject status in cerebrospinal fluid (graph a) normal-appearing white matter (graph b) and white matter lesions (graph c). A higher AUC value is consistent with higher BBB permeability. Mean values are shown to the right of subgroup data with standard error bars marked. *P* values represent Kruskal-Wallis test results comparing AUC values between subgroups.